STAINING OF PORCELAIN TILES: INFLUENCE OF FELDSPAR PARTICLE SIZE

H. J. Alves, F. G. Melchiades and A. O. Boschi*

Laboratório de Revestimentos Cerâmicos (LaRC)
Departamento de Engenharia de Materiais (DEMa)
Universidade Federal de São Carlos (UFSCar)
Rod. Washington Luiz, Km. 235, 13574-970
São Carlos, SP, Brazil

*e-mail: daob@ufscar.br

ABSTRACT

The staining of porcelain tiles is related to the presence of pores. The porosity of porcelain tiles results mainly from the incomplete elimination of the pores of the green compact during sintering. Consequently, to control the staining of porcelain tiles of a given composition it's important to pay special attention to the porosity of the green compact and the sintering conditions. Regarding the green compact, the volume and the morphological characteristics of intragranular and intergranular pores are dependent, among others variables, on the particle size distribution (PSD) of the raw materials and the pressing pressure. The elimination of these pores during sintering will take place through liquid phase sintering. The most important raw material responsible for the amount, nature and characteristics of the liquid phase during sintering, and consequently the capability of a composition to eliminate the green compact pores, is feldspar. The particle size distribution of the feldspar will affect the development of the green microstructure during compaction (volume and characteristics of the pores) and its reactivity during sintering. It is therefore a very important variable regarding the staining of porcelain tiles. The objective of the present work was to study the correlations between the PSD of feldspar, the characteristics of the pores in the green compact, the elimination of these pores during sintering and the susceptibility to staining of sintered polished surfaces. It was found that small variations in the average particle size of feldspar are capable of causing significant changes in the microstructure of the porous mass, and thus of modifying the resistance to staining of the porcelain tile polished surface.

1. INTRODUCTION

The porosity of porcelain tiles results from the incomplete densification of the material during the stages of processing.[1] In the green compact, the volume and morphological characteristics of intragranular and intergranular pores depend on the particle size distribution (PSD) of the raw materials, the granulometric distribution of the spray-dried material and the compaction pressure. The porosity of the green compact and the heat treatment applied during sintering determine the porous microstructure of the final product, and hence its properties.[2,3,4] However, the use of raw materials such as feldspar, with a high potential for forming liquid phase during sintering, contributes to eliminate porosity when a suitable heating cycle is employed.[5,6]

Porcelain tile staining is caused by the presence of pores. Therefore, controlling the staining of porcelain tiles of a given composition requires focusing special attention on the porosity of the green compact and on its sintering conditions.[7-10]

A recent study found that the granulometric distribution of spray-dried material does not interfere significantly in its pore size distribution after sintering, since distinct granulometric compositions led to the same porosity in the sintered product.[3] The milling yield of the porcelain bodies evaluated by AMORÓS[4] was related to the porosity of the green compact, the porosity of the final product and the stain resistance. The aforementioned study found that insufficient milling (larger residue on an ASTM #325 sieve) is responsible for producing green ceramic bodies with a wide pore size distribution and higher apparent density (higher packing). However, a wider pore size distribution implies the presence of pores with large diameters in the green compact, which impairs the sintering process because high temperatures are required to reach maximum densification, resulting in a product with low apparent density and low stain resistance.[1,2,4]

This work presents the results of a study that investigated the effect of the PSD of feldspar on the formation of pores in the green compact and the final product, using stain resistance as an evaluation parameter of surface porosity. To this end, the feldspar used in a standard body of technical porcelain was milled under different conditions to produce the desired changes in its PSD.

2. MATERIALS AND METHODS

This research used raw materials that make up the standard body (STD) of a commercial polished porcelain tile whose formulation and chemical analysis are presented in Tables 1 and 2, respectively. The STD body was evaluated previously by X-ray fluorescence (Philips MagiX spectrometer). Several of the parameters used here were determined based on the information provided by the manufacturer of the product and the literature on the subject. The methodology adopted was designed to reveal the effect of the addition of feldspar with different PSD profiles

on the properties of the STD body. Thus, because the main objective was to analyze the variable of PSD separately, the chemical and mineralogical compositions of the raw materials were not examined.

Raw materials	STD (in wt.%)	F1* (in wt.%)
Feldspar	**51.5**	-
Clay I	18.4	38.0
Kaolin	14.5	30.0
Clay II	4.9	10.0
Alumina	3.9	8.0
Zirconite	3.9	8.0
Frit	2.9	6.0

* Formulation F1 (without feldspar) was readjusted while maintaining the proportions of the other components of the STD body.

Table 1 – Formulation of the STD body and the F1 composition.

Oxides (%)	STD
L.O.I.	3.37
SiO_2	56.91
Al_2O_3	23.61
Fe_2O_3	0.28
TiO_2	0.10
CaO	1.07
MgO	0.43
K_2O	0.96
Na_2O	2.42
Li_2O	0.54
ZrO_2	10.16
P_2O_5	0.15

Table 2 – Chemical analysis of the STD body.

2.1. Milling of the standard body

The STD body was initially obtained by proportioning and mixing the raw materials previously dried at 110°C for 24 h, in the proportions listed in Table 1. This composition was milled in a laboratory ball mill (Certech ST-242) to obtain a suspension with 60% (m/m) of water and a milling residue of about 0.5% after sifting through an ABNT #325 sieve (parameter used by the manufacturer of the product). The milling time was 14 min and the other conditions of the experiment were standardized as follows: mill (1000 mL), load of alumina balls (600 g of large balls and 585 g of small balls), solids mass (300 g), water mass (180 g) and sodium silicate as a deflocculant (1.8 g). After milling was concluded, the mill was emptied and the density of the suspension (ρ_S) was determined using a stainless steel pycnometer (model 108 – tare 200). The suspension contained in the pyc-

nometer was then sifted through the ASTM #325 sieve to determine the milling residue by drying and weighing the particles retained on the mesh (> 45 μm). Part of the original suspension (sifted through the ASTM #250 sieve) was subjected to X-ray sedimentometry (Micromeritics Sedigraph 5000 D) to determine its PSD. The remainder of the suspension was dried in an electric oven at 110ºC for 24 h. After drying, the absolute density of the solids (ρ_R) was determined by helium pycnometry (Quantachrome Ultrapycnometer 1000).

2.2. Milling of the feldspar

The methodology applied in this phase of the work was divided into three stages:

Stage 1: The feldspar was milled individually under the same conditions as those described in item 2.1., using three different milling times (21.0 min, 18.5 min and 12.5 min) to obtain different residues on an ASTM #325 sieve. The resulting suspensions were analyzed to determine the ρ_S, ρ_R, milling residue and PSD.

Stage 2: Concomitantly, a STD suspension was prepared containing no feldspar, which was referenced F1. To this end, the STD composition was altered by excluding this raw material, and therefore required an adjustment, maintaining the proportions found originally among the other initial components, as indicated in Table 1. Composition F1 was milled for 12.0 min to obtain a residue of less than 0.5% retained on the ASTM #325 sieve, i.e. close to the amount of residue of the STD body. The values of ρ_S and ρ_R in F1 were determined.

Stage 3: After preparing the feldspar suspension under the milling conditions described in Stage 1, the procedure consisted of mixing the three different residues individually into the F1 suspension by means of quantitative volumetric addition to reproduce the initial STD formulation (Table 1). For this purpose the calculations were based on equation 1, where M_S is the dry mass of solids present in a given volume V_S of suspension.

$$M_S = V_S \cdot \rho_R \left(\frac{\rho_S - 1}{\rho_R - 1} \right) \quad (1)$$

Thus, knowing the mass of solids in a given volume of suspension, it was possible to determine the required volume of each suspension that should be mixed in order to reproduce the initial STD formulation.

Before and after each volumetric mixture, the suspensions were kept under mechanical shaking for 15 min, at a rotation of 800 rpm. Part of the volume of the suspensions was then analyzed to determine the PSD. The remaining volumes of these suspensions were dried at 110ºC for 24 h, and the resulting bodies were used for the preparation of green bodies.

2.3. Preparation and characterization of the green bodies

After drying the suspensions, the green bodies were prepared according to the procedures described below.

The solid materials were carefully ground in a porcelain mortar until they passed completely through an ASTM #42 sieve. They were then moistened with 0.060 kg water per kilogram dry material and granulated by sifting the powder through a sieve with 650 µm openings. The sieving procedure was repeated three times to ensure the homogeneity and quality of the granulation. The granulated powders were stored in separate plastic bags and allowed to "rest" for 24 h. For each evaluated condition, green bodies were prepared with dimensions of 6.0 x 2.0 cm by pressing the granulated powders under a uniaxial pressure of 44 MPa. The green bodies were dried at 110ºC until they reached a constant weight, after which they were analyzed by the geometric method to determine their apparent density (ρ_C), and by mercury porosimetry (Micromeritics AutoPore III) to characterize their porosity.

2.4. Sintering, characterization of the final porosity and evaluation of staining

The green bodies were sintered in an electric lab furnace, using a heating cycle of approximately 55 min, a heating rate of 45ºC/min, a dwell time of 8 min at the maximum temperature, and a cooling rate of 60ºC/min to room temperature.

The sintering temperature ($T_{máx}$) of the green bodies of each evaluated condition was chosen according to its maximum densification, based on the highest linear firing shrinkage (LS) and lowest water absorption (WA) presented at four different previously selected temperatures.

The following values were determined after sintering:

- WA, by the boiling water method for during two hours, according to the ISO 10545-3 standard[11];
- apparent porosity (ε_A) by the Archimedes principle;
- total porosity (ε) and closed porosity (ε_F), by means of equations:

$$\varepsilon = 1 - \left(\frac{\rho_{CS}}{\rho_{RS}} \right) \quad (2)$$

$$\varepsilon_F = \varepsilon - \varepsilon_A \quad (3)$$

where ρ_{CS} is the apparent density and ρ_{RS} the absolute density of the solid obtained after sintering; and

- degree of densification (ϕ), defined as:

$$\phi = \left(\frac{\rho_{CS}}{\rho_{RS}} \right) \quad (4)$$

Ten test specimens of each green body evaluated were used for the porosity tests.

Small samples were then precision cut from the sintered compacts, using a diamond cutting disc. These samples were cleaned ultrasonically for 20 min and dried at 110ºC for 24 h, after which they were sandpapered and polished using an automatic system with water, composed of a rotary disc and a series of five polishing pads to simulate the industrial polishing process. The samples were polished for 15 min with each pad, resulting in surfaces prepared under the same conditions.[12-14]

The characteristics of the samples' surface microstructure after polishing were determined from digital images (micrographs) obtained with a scanning electron microscope (SEM, Leo Stereoscan 440). The micrographs were analyzed using the Image-Pro 4.5 software program, which allowed determination of the percentage corresponding to the area covered by pores in relation to the total area of the analyzed images, their diameter distribution, and aspects related to their morphology (aspect ratio).

Concomitantly, several polished test specimens were subjected to stain resistance testing, according to the procedures of the ISO 10545-14 standard.[15] The staining agents used here were chrome green (an oily solution containing 40 wt.% of Cr_2O_3 – as recommended by the standard) and earth (an aqueous solution containing 50 wt.% of red earth – simulating conditions found in everyday situations).

The intensity of the stains was evaluated from the difference in colour ΔE*, of the surface prior to staining and after the cleaning steps applied on the region where the staining agents had been applied.[16] The values of ΔE* were determined by diffuse reflectance spectrophotometry (Konica Minolta CM – 2600d), using a standard 10º colorimetric observer and a standard D65 light source (equivalent to daylight). The higher the value of ΔE* the more intense the stain observed on the surface. Determination of stain intensity by spectrophotometry has proved very efficient in the evaluation of the staining tendency of ceramic tiles, according to recent works.[9,14,17]

It should be noted that the test specimens selected for the SEM analysis were the ones sintered at the temperature at which the highest densification of the material was reached (item 3.4).

3. RESULTS AND DISCUSSION

3.1. Milling parameters and characteristics of the suspensions

Table 3 describes the milling parameters used in the preparation of the suspensions with different residues and the resulting values of ρ_S and ρ_R. Note that, as the milling time increases, the amount of particle residues retained on the ASTM #325 sieve decrease, indicating the increasing degree of comminution achieved. The density of the suspensions, ρ_S, did not show major variations, since the volume of water and the mass of solids used in their preparation were constant.

As mentioned in item 2.2, the feldspar suspensions were mixed with suspension F1. The exact volume of each mixed suspension was calculated based on equation 1, using the values of ρ_S and ρ_R listed in Table 3. To facilitate the identification of the suspensions obtained after completing the mixtures, the following acronyms were established:

- **Fdsp 2.1%**: feldspar suspension with 2.1% of residue added to suspension F1;
- **Fdsp 4.3%**: feldspar suspension with 4.3% of residue added to suspension F1;
- **Fdsp 8.9%**: feldspar suspension with 8.9% of residue added to suspension F1.

In addition, the suspension of the STD body with 0.5% of residue was referenced: **Mass 0.5%**.

Suspensions	Milling time (min)	Residue on ASTM #325 sieve (in wt.%)	ρ_S (g/cm³)	ρ_R (g/cm³)
STD	14.0	0.5	1.66	2.835 ± 0.001
Feldspar	21.0	2.1	1.67	2.898 ± 0.002
	18.5	4.3	1.66	
	12.5	8.9	1.66	
F1	12.0	0.5	1.65	2.853 ± 0.001

Table 3 – Milling parameters and properties of the suspensions.

3.2. Effect of milling on PSD

As the milling time increases, the average size of the particles that make up a ceramic body should be reduced, leaving behind smaller amounts of residue on the ASTM #325 sieve. Figure 1a depicts the PSD graph obtained for the mixture of the suspensions with different amounts of feldspar residues (Fdsp 2.1%, Fdsp 4.3% and Fdsp 8.9%) and for the suspension of the standard body (Mass 0.5%). Note that increasing the degree of milling (lower residue on the ASTM #325 sieve) causes the average size of the feldspar particles to decrease.

Table 4 describes the main evaluation parameters of the PSD curves, among which D_{50} stands out for being a statistical parameter that represents the mean particle diameter when the percent cumulative mass is equal to 50%. The highest values of D_{50} are associated with a lower efficiency reached in the milling process.

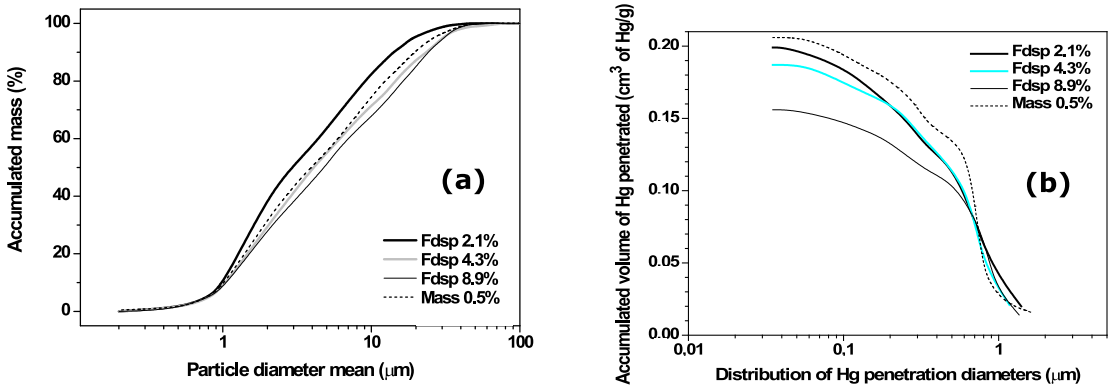

Fig. 1 – (a) PSD of feldspar milled in different residues on ASTM #325 sieve. Comparison against the standard Mass 0.5%; (b) Distribution of the mercury intrusion diameters in the green test specimens.

Suspensions	D_{50} (μm)	<10 μm (%)	<1 μm (%)
Mass 0.5%	**3.9**	**74.5**	**8.5**
Fdsp 2.1%	3.0	82.5	9.0
Fdsp 4.3%	4.1	72.5	8.1
Fdsp 8.9%	4.8	67.7	7.8

Table 4 – Evaluation parameters of the PSD curves according to Figure 1.

3.3. Effect of PSD on the green microstructure

Figure 1b presents the graphs obtained by mercury porosimetry, while Table 5 lists the values of apparent density (ρ_C) of the green test specimens and the volume of Hg intruded in each evaluated condition.

Green test specimens	ρ_C (g/cm³)	Cumulative volume of intruded Hg (cm³ of Hg/g)
Mass 0.5%	1.67 ± 0.01	0.206
Fdsp 2.1%	1.68 ± 0.01	0.199
Fdsp 4.3%	1.69 ± 0.01	0.197
Fdsp 8.9%	1.70 ± 0.01	0.156

Table 5 – Values of apparent density (ρ_C) and cumulative volume of intruded Hg.

A comparison of the Hg porosimetry curves (Fig. 1b) and the PSD curves (Fig. 1a) indicates that the use of different PSD for a given ceramic body significantly alters the pore volume of the green test specimens produced by compaction. In this context, the data in Table 5 confirm that the increase in the value of D_{50} (Table

4) is accompanied by a discrete increase in ρ_C and a decrease in the volume of Hg intruded in the test specimens. In other words, the use of suspensions containing coarser feldspar particles contributes to increase the degree of densification of the green compact, since the volume of pores generated is lower and ρ_C is higher.

These results are consistent with reports in the literature and confirm that the use of larger particles increases the apparent density of the green compact. This is due to the more efficient packing of this type of particle inside the granules during the granulation stage (item 2.3), favouring the obtainment of granules with a smaller volume of intragranular pores.

As for the distribution of diameters of Hg intrusion, it was found that the Fdsp 2.1%, Fdsp 4.3%, Fdsp 8.9% and Mass 0.5% test specimens presented similar profiles, although the volume of intruded Hg differed (Fig. 1b). This indicates that the distinct feldspar milling conditions used in this work led to greater changes in the volume of pores in the green compacts than in the distribution their diameters.

3.4. Sintering of the test specimens

The test specimens were sintered at four different temperatures and evaluated to determine the degree of densification attained by each one. Gresification curves were built (Fig. 2) based on the values of AA and RLq obtained, and the following $T_{máx}$ were selected: Mass 0.5% = 1200°C; Fdsp 2.1% = 1230°C; Fdsp 4.3% = 1230°C; and Fdsp 8.9% = 1250°C.

With regard to the standard body (Mass 0.5%), the use of coarser feldspar particles (Figure 2) caused a gradual increase in the $T_{máx}$, making it less reactive. Because the densification process during sintering of the porcelain body involves the formation of liquid phase, the larger the size of feldspar particles the smaller the free specific surface that participates in the sintering process, which increases the maximum densification temperature of the material.

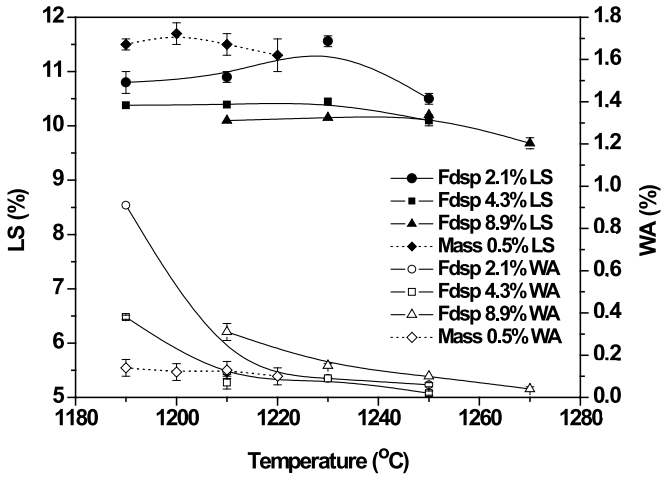

Figure 2 – Variation of linear shrinkage (LS) and water absorption (WA) with sintering temperature of the test specimens.

3.5. Physical characterization of the sintered test specimens

The test specimens subjected to physical characterization were the ones sintered at $T_{máx}$, which was determined based on the gresification curves (Fig. 2).

Table 6 presents the values of WA,LS , ε_A ,ε_F , ε and ϕ of the analyzed test specimens. Comparing the porosity of the standard Mass 0.5% with that presented by Fdsp 2.1%, it is clear that the Fdsp 2.1% test specimens exhibit lower values of ε_F and ε, and slightly higher ϕ, despite their higher content of feldspar milling residue. Among the compositions with different feldspar milling residues, the results show that the use of coarser particles causes the LS to decrease and the ε_F to increase. This indicates that the decrease in the degree of densification ϕ of the test specimens is a result of the lower reactivity obtained in sintering.

A comparison of the characteristics of the green compacts (Table 5) with the results obtained for the sintered test specimens (Table 6) reveals that the bodies that initially presented the highest pore volumes were the ones that reached the highest degree of densification during sintering. This is due to the fact that, although the use of fine particles is the main cause for lower packing of the green compact, during sintering this type of particle enhances the reactivity of the material and of the content of the liquid phase, contributing to the process of densification.

Test specimens	WA (%)	LS (%)	ε_A(%)	ε_F (%)	ε[a] (%)	ϕ
Mass 0.5%	0.12 ± 0.04	11.7 ± 0.2	0.21 ± 0.09	9.42 ± 0.12	9.63 ± 0.10	0.92
Fdsp 2.1%	0.09 ± 0.00	11.6 ± 0.1	0.22 ± 0.05	8.44 ± 0.07	8.66 ± 0.06	0.93
Fdsp 4.3%	0.09 ± 0.00	10.5 ± 0.0	0.21 ± 0.06	10.60 ± 0.07	10.81 ± 0.07	0.91
Fdsp 8.9%	0.10 ± 0.00	10.2 ± 0.0	0.26 ± 0.10	12.91 ± 0.10	13.17 ± 0.10	0.89

[a] The value of ρ_R obtained for the calculation of ε was 2.690 g/cm³.

Table 6 – Physical characterization of the sintered test specimens.

3.6. Analysis of SEM images and staining

Figure 3 presents the SEM micrographs of the surfaces of the polished test specimens.

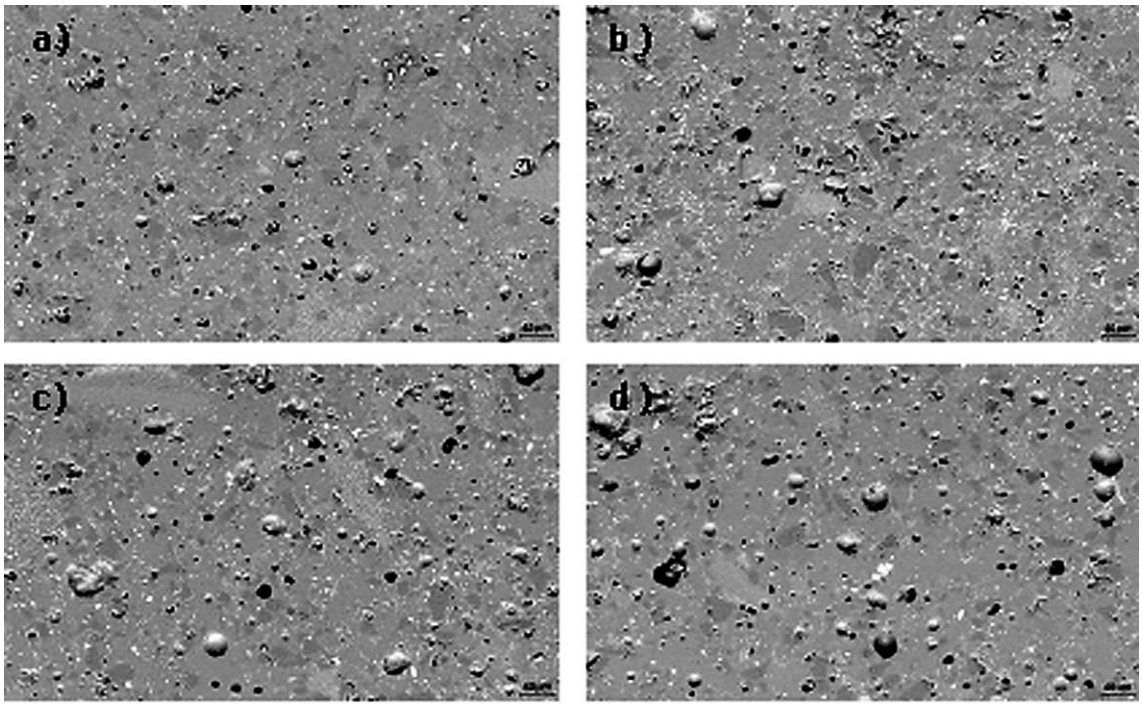

Figure 3 – SEM micrographs of the surfaces of the polished test specimens: (a) Mass 0.5%, (b) Fdsp 2.1%, (c) Fdsp 4.3%, and (d) Fdsp 8.9%.

The results of the image analysis were organized on graphs of pore diameter distribution (Fig. 4a) and aspect ratio (Fig. 4b) as a function of cumulative percent of pores. Table 7 lists the percent of pores per unit area of the polished surface with the values of ΔE* after the stain resistance test.

Based on the results of the analysis of the images and staining, the following aspects deserve highlighting:

- Among the Fdsp bodies, the least effective milling of feldspar contributed to a discreet increase in the average pore diameter observed in the sintered material. This tendency was accompanied by an increase in the space occupied by pores in relation the area in the images as the milling residue increased. The values of ΔE* were also found to increase along with the increase in milling residue, i.e. surface cleanability is impaired by the decrease in the degree of milling.

- Upon comparing the results of stain resistance of the Fdsp bodies with the standard Mass 0.5% body, one finds that the Fdsp 2.1% composition presented a slightly better stain resistance than the standard, since the ΔE* values obtained were lower. This indicates that less controlled milling of feldspar, with residues of up to 2.1% on the ASTM #325 sieve, is feasible. In this case, the values of ΔE* seem to depend more on the pore area than on their dia-

meter distribution and morphology. This based on the fact that, although the surfaces of Mass 0.5% presented pores with smaller diameters (Fig. 4a) and shapes tending toward the spherical (Fig. 4.b), the polished surfaces of the Fdsp 2.1% test specimens showed the best result, i.e. the lowest percent of pores per unit area.

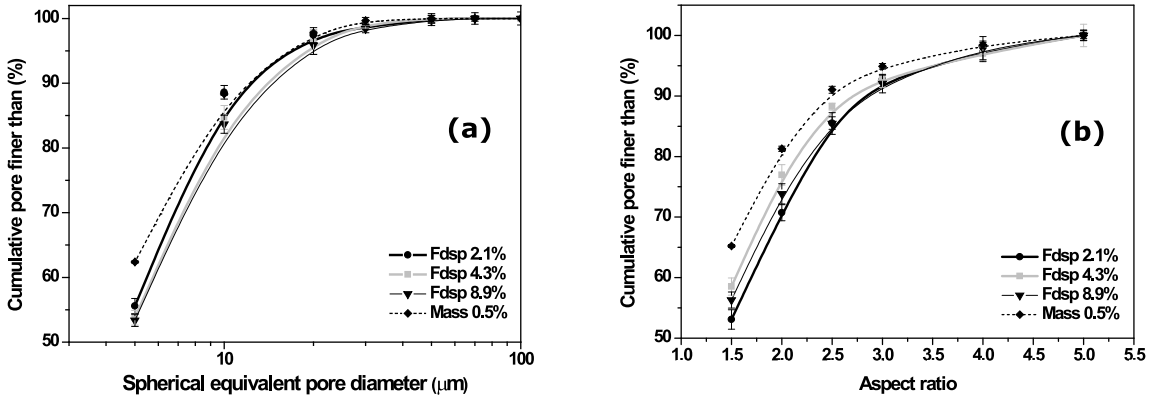

Figure 4 – (a) Pore diameter distribution on the surface of the polished test specimens; (b) Distribution of the values of the aspect ratio of pores on the surface of polished test specimens.

Polished test specimens	Pores per unit area (%)	ΔE*
Mass 0.5%	4.51 ± 0.40	1.93
Fdsp 2.1%	4.32 ± 0.76	1.34
Fdsp 4.3%	5.51 ± 0.64	5.77
Fdsp 8.9%	6.71 ± 0.93	6.12

Table 7 – Results of image analysis and ΔE.*

3.7. Relationship between the PSD of feldspar and post-sintering properties

To facilitate the interpretation of the results, a graph was created to evaluate the individual participation of feldspar in the formation of closed pores and staining (Fig. 5).

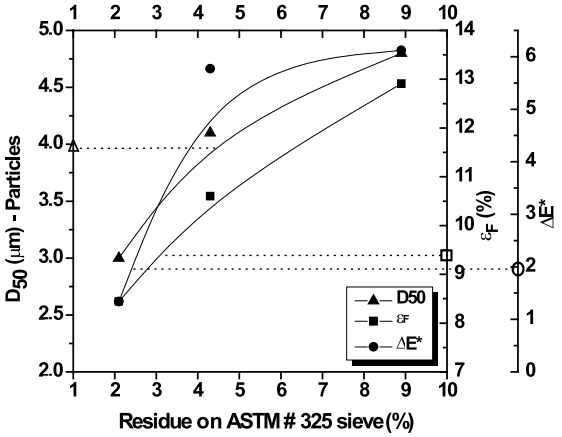

Figure 5 – Variation of D_{50}, and ΔE according to feldspar milling residues. Highlighted points on the axes: values presented by the Mass 0.5% standard.*

As can be seen in Figure 5, the decrease in the degree of milling of feldspar causes an increase in the average size of the particles that will make up the granules of the material. Although the degree of densification of the green compact is higher in these conditions, the increase in D_{50} is accompanied by an increase in the percentage of closed pores due to the lower reactivity of the body during sintering. Polishing the sintered test specimens reveals the closed pores at the surface and acts negatively on the stain resistance of the specimens, increasing the intensity of stains as the number of pores increases (higher percentage). It was found that a minor variation in feldspar milling residue can significantly alter the pore volume and cleanability of the polished surface.

4. CONCLUSIONS

The results of this work led to the following conclusions:

- The degree of densification of the green compact may vary according to the PSD of the raw materials that make up the feldspar body. As the milling time decreases, the average particle size increases, favouring the formation of denser granules during the granulation stage. In such conditions, the green compact reaches higher values of apparent density due to the reduction of its intragranular pore volume. However, the use of particles with larger diameters causes the volume and diameter of closed pores to increase due to the lower reactivity attained during sintering, thus worsening the cleanability of the polished surface.
- Slight variations in the average particle size of feldspar can lead to significant changes in the porous microstructure of the final product, thereby modifying its stain resistance. Under the conditions adopted in this work, it is possible to incorporate feldspar in a porcelain body with a milling residue of up to 2.5% retained on an ASTM #325 sieve (according to the tendency illustrated in Fig. 5), without impairing the product's stain resistance, and even achieve a discrete reduction in the intensity of staining when compared with the STD body.

REFERENCES

[7][1] Dondi, M., Raimondo, M., Zanelli, C. Stain resistance of ceramic tiles. *Ceramic World Review*, 2008, **77**, 82-89.

[8][2] Cavalcante, P. M. T., Dondi, M., Ercolani, G., Guarini, G., Melandri, C., Raimondo, M., Amendra, E. The influence of microstructure on the performance of white porcelain stoneware. *Ceramics International*, 2004, **30**, 953-963.

[9][3] Dondi, M., Ercolani, G., Guarini, G., Melandri, C., Raimondo, M., Rocha and Almendra, E., Cavalcante, T. P. M. The role of surface microstructure on the resistance to stains of porcelain stoneware tiles. *Journal of the European Ceramic Society*, 2005, **25**, 357-365.

[10][4] Alves, H. J., Minussi, F. B., Melchiades, F. G., Boschi, A. O. Characteristics of pores responsible for staining of polished porcelain tile. *Industrial Ceramics*, 2011, **31**, 21-26.

[1][5] Beltrán, V., Ferrer, C., Bagán, V., Sánchez, E., Garcia, J., Mestre, S. Influence of pressing powder characteristics and firing temperature on the porous microestructure and stain resistance of porcelain tile. In *Proceedings of the IV World Congress on Ceramic Tile Quality. Cámara Oficial de Comercio y Navegación*, 1996, 133-148.

[2][6] Amorós, J. L., Cantavella, V., Jarque, J. C., Felíu, C. Fracture properties of spray-dried powder compacts: effect of granule size. *Journal of the European Ceramic Society*, 2008, **28**, 2823-2834.

[3][7] Alves, H. J., Melchiades, F. G., Boschi, A. O. Effect of spray-dried powder granulometry on the porous microstructure of polished porcelain tile. *Journal of the European Ceramic Society*, 2010, **30**, 1259-1265.

[4][8] Amorós, J. L., Orts, M. J., García-Ten, J., Gozalbo, A. and Sánchez, E., Effect of the green porous texture on porcelain tile properties. *Journal of the European Ceramic Society*, 2007, **27**, 2295-2301.

[5][9] Martín-Márques, J., Rincón, J. Ma., Romero, M. Effect of firing temperature on sintering of porcelain stoneware tiles. *Ceramics International*, 2008, **34**(8), 1867-1873.

[6][10] Suvaci, E., Tamsu, N. The role of viscosity on microstructure development and stain resistance in porcelain stoneware tiles. *Journal of the European Ceramic Society*, 2010, **30**, 3071-3077.

[11][12] International Standard ISO 10545-3, Ceramic Tile – Part 3: Determination of water absorption, apparent porosity, apparent relative density and bulk density, 1997.

[12][13] Hutchings, I. M., Xu, Y., Sánchez, E., Ibáñez, M. J., Quereda, M. F. Porcelain tile microstructure: implications for polishability. *Journal of the European Ceramic Society*, 2006, **26**, 1035-1042.

[13][14] Jazayeri, S. H., Salem, A., Timellini, G., Rastelli, E. A kinetic study on the development of porosity in porcelain stoneware tile sintering. *Boletin de la Sociedad Española de Cerámica y Vidrio*, 2007, **46**(1), 1-6.

[14][15] Alves, H. J., Freitas, M. R., Melchiades, F. G., Boschi, A. O. Dependence of surface porosity on the polishing depth of porcelain stoneware tiles. *Journal of the European Ceramic Society*, 2011, **31**, 665-671.

[15][16] International Standard ISO 10545-14, Ceramic Tiles – Part 14: Determination of resistance to stains, 1997.

[16][17] Rastelli, E., Tucci, A., Esposito, L., Selli, S. Stain resistance of porcelain stoneware tile: mechanisms of penetration of staining agents and quantitative evaluation. *Ceram. Acta*, 2002, **14**(1), 30-37.

[17][18] Sánchez, E., Ibáñez, M. J., García-Ten, J., Quereda, M. F., Hutchings, I. M., Xu, Y.M. Porcelain tile microstructure: implications for polished tile properties. *Journal of the European Ceramic Society*, 2006, **26**, 2533-2540.